Theor Chem Acc (2001) 106:393–403
DOI 10.1007/s002140100295

Theoretical
Chemistry Accounts

*Regular article*

# Ab initio study of bonding trends for $f^0$ actinide oxyfluoride species

**Michal Straka**[1], **Kenneth G. Dyall**[1,2], **Pekka Pyykkö**[1]

[1] Department of Chemistry, University of Helsinki, POB 55 (A. I. Virtasen aukio 1), 00014 Helsinki, Finland
[2] Eloret Corporation, 690 W. Fremont Ave. Suite 8, Sunnyvale, CA 94087, USA

Received: 18 May 2001 / Accepted: 21 June 2001 / Published online: 11 October 2001


**Abstract.** Fully relativistic, four-component Dirac–Fock calculations and quasirelativistic pseudopotential calculations at different ab initio levels are used to study the bonding trends among the naked, triatomic $[OAnO]^{q+}$ groups or the oxyfluorides $[AnO_nF_m]^q$ with $f^0$ configurations. The triatomic $f^0$ series is suggested to range from the bent $ThO_2$ via the linear $OPaO^+$ to at least $NpO_2^{3+}$, a possible new gas-phase species. The neutral oxyfluoride molecules include the experimentally unknown $NpO_2F_3$ and $PuO_2F_4$. The latter is a candidate for the so far unknown oxidation state Pu(VIII), which is found to lie considerably above Pu(VI), but to be locally stable. Their all-oxygen isoelectronic analogues are $NpO_5^{3-}$, known in the solid state, and the unknown $PuO_6^{4-}$. Further possible candidates for Pu(VIII) are $PuO_4(D_{4h})$ and the cube-shaped $PuF_8(O_h)$. Isoelectronic $UF_8^{2-}$ is calculated to be $D_{4d}$, in agreement with experiment.

**Key words:** Actinyls – Neptunium(VII) – Plutonium(VIII) – Structure chemistry – Relativistic Quantum Chemistry

## 1 Introduction

Owing to their complicated hybridization, actinides are a fascinating subject for theoretical studies. One purpose of such calculations is to use complete maps of isoelectronic series to identify so far unknown chemical species. As an example, the uranyl analogue $NUO^+$, predicted in Ref. [1], was observed by mass spectroscopy and reported in Ref. [2]. Later it was prepared in neon matrices as well [3]. The trends of bond lengths or force constants along such isoelectronic series will then give an indication on the stability of the various species. A general review of actinide chemistry, is given in Ref. [4]. The latest specific reviews on the structure and spectra of actinyl compounds appear to be those by Denning [5, 6] and Glebov [7]. The quantum chemical calculations on actinide compounds have been recently reviewed [8–12]. The original articles can be found from Refs. [13–15].

On the experimental side concerning the triatomic, $f^0d^0$ $OAnO^q$, actinyl series, $ThO_2$ has been seen in both molecular beams [16] and argon matrices [17, 18]. It was shown to be bent. The protactinyl group $PaO_2^+$ is known in protactinium chemistry [19]. The uranyl group $UO_2^{2+}$ is one of the most common species in uranium chemistry. The bare uranyl ion has been seen in the gas phase [20] and possibly in rare-gas matrices [21]. Recent work has, however, reassigned this absorption to $UO_2^+$ [21b]. The green $f^0$ neptunyl(VII) species, with a number of equatorial ligands, has been known since the late 1960s [22]. No Pu(VIII) compounds in any form are known.

Our aim here is to see what possible new species remain to be discovered; hence, the approach has to be encyclopedic. A complete map of the possible $f^0d^0[AnO_2F_n]^q$ actinyl fluoride species is shown in Fig. 1 and their general structures are shown in Fig. 2. Of them, neutral $UO_2F_2$ and also $UOF_4$ have been seen in matrices [23]. Of the charged complexes, $UO_2F^+$ is known [24]. The entire $[UO_2F_n]^{2-n}$ series for $n = 1 - 5$ has been observed by NMR spectroscopy in aqueous solution [25]. The equatorially pentacoordinated $UO_2F_5^{3-}$ occurs in solids [26]. In addition, thermochromatographic evidence has been presented for the $f^0$ species $UOF_4$, $UO_2F_2$, $NpF_7$ and $NpO_3F$ by Fargeas et al. [27].

On the theoretical side, starting with the actinyls, various members of the dipositive $OAnO^{2+}$ series, notably their optical spectra, have recently been theoretically studied [28, 29]. In this series, for An = U–Am, the shortest bond length occurred at Am [28, 30]. For tripositive $ONpO^{3+}$, nonrelativistic scattered-wave $X-\alpha$ calculations at a fixed bond length exist [31]. The $[UO_2X_4]^{2-}$ series was recently considered by Schreckenbach et al. [32]. Isoelectronic -N=U=N- analogues were studied by Kaltsoyannis [33]. Triatomic uranium $XUY$ species ($X, Y$ = C,N,O) were studied recently [34].

*Correspondence to*: P. Pyykkö
e-mail: pekka.pyykko@helsinki.fi

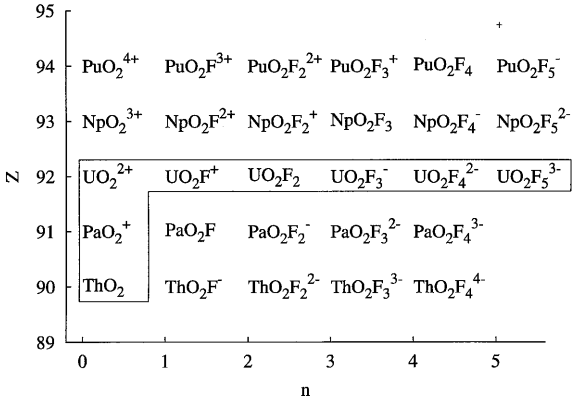


**Fig. 1.** A map of possible $f^0$ $[AnO_2F_n]^q$ species

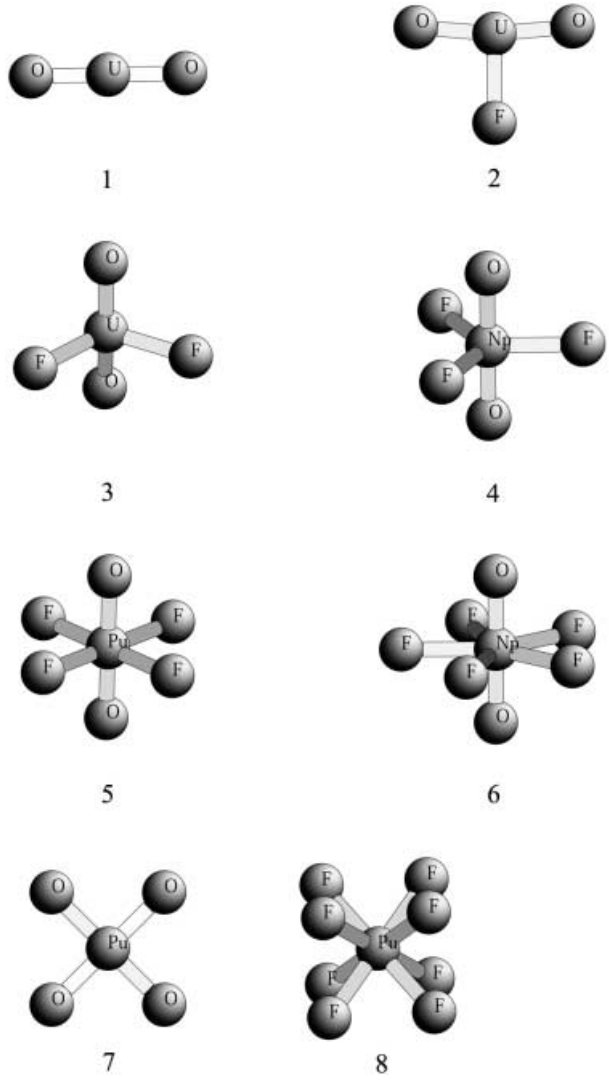


**Fig. 2.** Structures of species calculated in this work (at the B3LYP level)

Beyond the $f^0d^0$ maximum oxidation states we have recently made the admittedly bold proposal of formally oxidizing electrons from the 6*p* semicore shell. Ultimately this would lead to an octahedral, high-energy uranium(XII) hexoxide molecule [35]. It would also be remarkable because so far the highest known oxidation state of any element appears to be +VIII, which occurs for example, in the $d^0$ species $OsO_4$ or $RuO_4$. Among the known actinide compounds, those with the highest known oxidation state appear to be the $f^0$ Np(VII) compounds. Attempts to make Pu(VIII) compounds have so far failed. Some entirely new chemical questions to be addressed are

- Can plutonium(VIII) exist? Despite numerous experiments, no ab initio calculations are available.
- Could the known neptunium(VII) exist in neutral, highly symmetrical molecules, such as $NpO_2F_3$?
- What are the structures of experimentally known $NpO_5^{3-}(s)$ and $NpO_3F(g)$ species?
- Is the observed $D_{4d}$ structure of the $UF_8^{2-}$ anion in $(NO)_2(UF_8)$ [36] of intramolecular origin? How about the structure of isoelectronic $PuF_8$?

## 2 Results and discussion

### *2.1 Actinyls*

#### 2.1.1 Bonds and bond lengths

Calculated structures for $f^0$ dioxoactinides from $ThO_2$ to $PuO_2^{4+}$ are summarized in Table 1. The next species, $AmO_2^{5+}$, blows up at quasirelativistic Hartree–Fock (QR-HF) and Dirac–Fock (DF) levels, and was not studied in detail. At the lighter end, $AcO_2^{-}$ would be bent, O–A–O = 112.8°, An–O 207.1 pm, frequencies 636($a_1$), 559($b_2$), 170($a_1$) at the B3LYP level. This was also not studied in detail.

As seen from Table 1, the pseudopotential QR-HF and the full DF calculations agree closely. The QR-HF bond length deviates from the DF one by 2 pm or less, while the relativistic small-core (RSC) effective core potential (ECP) performs slightly better then the relativistic large-core (RLC) ECP. A problematic case is $PaO_2^{+}$, where both the RLC and the RSC calculations differ by about 2 pm from the DF ones and the difference of 4.3 pm between them is alarming (for other actinides the values agree within 1.2 pm). A possible reason is the Pa ECP. A comparison with the correlated four-component calculations on uranyl and the experimental bond angle for thoryl shows reasonable agreement, (Table 1, Fig. 3). As we move from Th to Pu the An–O distance becomes shorter and shows a minimum near Pu for the QR-HF and DF methods, with an *R* of 158 pm for $PuO_2^{4+}$, (Fig. 3, Table 1).

The influence of electron correlation effects on *R* increases when going from $ThO_2$ to $PuO_2^{4+}$, and is exaggerated at the MP2 level. The most fundamental method here is CCSD(T) and the B3LYP results are close to it. A closer analysis of the underlying reasons is interesting. When moving from Th to Pu the virtual *f* and *d* shells come down, closer to the occupied orbitals, which may lead to the multiconfigurational character.

Thus, both the neptunyl and plutonyl systems become increasingly multiconfigurational. If the static

**Table 1.** Calculated An–O distances (pm) for $AnO_2^{n+}$ singlet species. Series from Th to Pu. For the bent systems the An–O–An angle (degrees) is given in *parentheses*

| Method | $ThO_2$ | $PaO_2^+$ | $UO_2^{2+}$ | $NpO_2^{3+}$ | $PuO_2^{4+}$ |
|---|---|---|---|---|---|
| RLC[a] | | | | | |
| HF | 189.7 (122) | 171.9 | 163.1 | 158.0 | 157.8 (161.8) |
| B3LYP | 190.4 (133) | 175.2 | 168.4 | 166.5 (156.3) | f |
| MP2 | 193.4 (116) | 178.2 | 171.9 | 177.6 | f |
| CCSD(T) | 192.8 (121) | 176.9 | 169.6 | 167.3 | 191.2[g] |
| RSC[b] | | | | | |
| HF | 188.9 (120) | 176.1 | 164.2 | 159.1[l] | 157.3 |
| B3LYP | 190.0 (119) | 180.0 | 169.5 | 166.8 (164) | 171.2 (168.8) |
| MP2[d] | 191.9 (113) | 182.4 | 172.4 | 175.7 | f |
| MP2[e] | 191.6 (113) | 182.1 | 172.8[j] | 175.8 | f |
| CCSD(T) | 191.5 (122[k]) | 181.2 | 170.2[j] | 168.2 | 178.0[g] |
| CASSCF | | | | 167.8[h], 168.5[i] | f |
| All electron[c] | | | | | |
| DF | 189.8 (120) | 174.2 | 165.0 | 159.8 | 158.4 |

[a] Basis set: An(RLC + 2*g*) + O(aug-cc-PVDZ)
[b] Basis set: An(RSC + 2*g*) + O(aug-cc-PVDZ)
[c] Basis set of aug-cc-PVDZ quality on both An and O
[d] Oxygen 1*s* not correlated
[e] Oxygen 1*s* and An 5*spd* not correlated
[f] No minimum found
[g] Forced to be linear
[h] CAS(12e/12orb)
[i] CAS(12e/16orb)
[j] The 4-MP2 values is 173.9 pm and the 4-CCSD(T) value is 171.5 [58]
[k] The experimental value is 122.5° [59]
[l] The calculated Np–O distance is 160 pm [41]

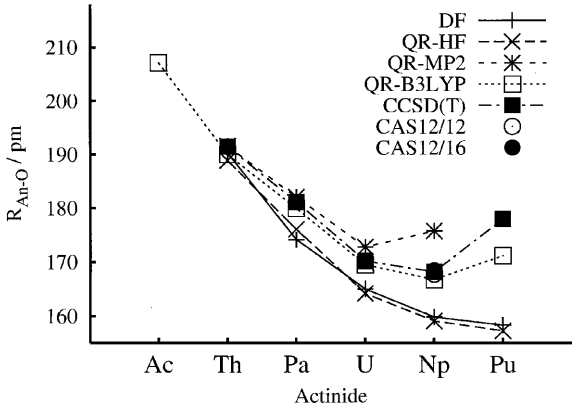


**Fig. 3.** Actinide–oxygen distances for the $f^0$ $OAnO^q$ species

correlation is included at the complete-active-space (CAS) level (12electrons/12orbitals), $NpO_2^{3+}$ survives with an Np–O distance of 167.8 pm, which is close to the CCSD(T) value of 168.2 pm. At the minimum geometry, the ground state is contaminated by the 5*f* orbitals. The weight of the "pure 5*f*" lowest unoccupied molecular orbitals (LUMO) becomes about 10%. An increase of the correlation space for the CAS to 12electrons/16orbitals or 10electrons/16orbitals, or a further increase of the basis set does not change the picture (Fig. 3, Table 1). For the $PuO_2^{4+}$ case, Pu is already too "hungry" for *f* electrons. Starting from the HF minimum of 158 pm, using CAS(12electrons/16orbitals or smaller) the low-lying *f* orbitals become strongly occupied and the system disintegrates. The large T1 diagnostic of 0.035 for a CCSD(T) calculation on $PuO_2^{4+}$ also suggests the multireference nature of that theoretical system. The CCSD(T) results may be irrelevant for $PuO_2^{4+}$ , while they still survive for $NpO_2^{3+}$ (with T1 = 0.022). For these reasons the MP2 distances overshoot and the frequencies are underestimated. Hence the MP2 method probably does not give reliable results beyond uranyl for the triatomic species. A multireference nature may also explain some bending tendencies which are seen for B3LYP calculations on $NpO_2^{3+}$ and $PuO_2^{4+}$, (Table 1). All the problems mentioned are more pronounced for RLC calculations. Qualitatively the lowering of the "pure 5*f*" levels from U to Np to Pu is reflected in the colors of these compounds. Uranyl compounds are yellowish and $NpO_2^{3+}$ compounds are green. Both transitions involve excitations from the occupied MOs to the lowest pure *f* levels. The $f^1$ $PuO_2^{3+}$ compounds are blue–black [31, 37]. Owing to the complexity of the system, no attempt was made to localize the transition state between the $D_{\infty h}$ minimum of $NpO_2^{3+}$ and the Coulomb asymptotes.

### 2.1.2 Nature of bonding

A perennial question is that of the An hybridization, in particular concerning the 6p$\sigma$ hole. From Fig. 4 we see that this hole increases along the An series and reaches a maximum at about −0.5 around Np and Pu, using Mulliken population analysis at the B3LYP minimum. The 5*f* character in the covalent bonds steadily increases from Th to Pu, while the 6*d* character stays almost constant. Bending of the molecules increases the 6*d* population, which is favorable for $ThO_2$, but not for the higher members of the series [30].

The four bonding MOs and two lowest empty MOs of $NpO_2^{3+}$ are shown in Fig. 5. They entirely correspond to one's intuitive notion of the $6d\sigma_g$ and $6d\pi_g$ or $5f\sigma_u$

and $5f\pi_u$ bonding. Figure 5 also shows the shape of the $5f\delta_u$ LUMO and the next MO, $5f\phi_u$, which was thought to play a major role in equatorial bonding of the actinyls (see later).

### 2.1.3 Frequencies

Calculated harmonic vibrational frequencies for the $OAnO^q$ series are shown in Table 2. The trends of the symmetric and antisymmetric O–An–O stretching vibrations are plotted in Figs. 6 and 7, respectively. The $\sigma_u$ value for $ThO_2$ agrees well with experiment, the $\sigma_g$ value less so. For calculated free $UO_2^{2+}$ the B3LYP and CCSD(T) $\sigma_u$ frequencies cluster above 1100 $cm^{-1}$. The symmetric stretching frequencies in Fig. 6 exhibit similar trends as the antisymmetric ones. Now we can further calibrate the QR-ECP calculations against fully relativistic, four-component all-electron calculations at the MP2 and CCSD(T) levels. We emphasize the role of electron correlation effects in lengthening the actinyl bonds and decreasing the vibrational frequencies. The all-electron DF calculations are helpful in calibrating the pseudopotential calculations, but can not be used to claim the existence of $PuO_2^{4+}$, for instance. The HF/DF agreement also suggests that spin–orbit effects are not essential at the HF level.

The suggested gas-phase species $NpO_2^{3+}$ should have similar $\sigma_g$ and $\sigma_u$ frequencies as $UO_2^{2+}$, at the CCSD(T) level, but a clearly smaller $\pi_u$ frequency. As seen from Table 3 the $UO_2^{2+}$ and $NpO_2^{3+}$ stretching frequencies are indeed comparable with each other. For both species, the values decrease from the free cation, when equatorial ligands (discussed later) are added. The calculated

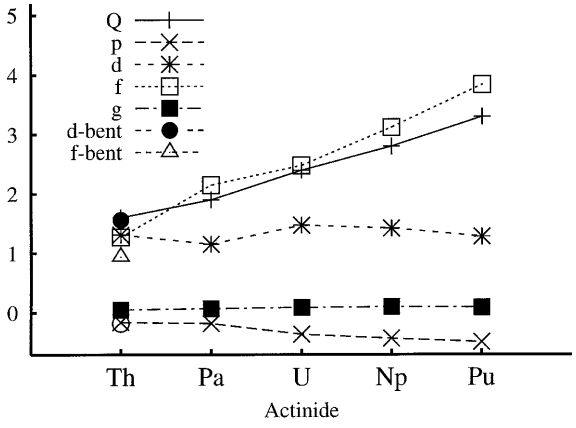


**Fig. 4.** The orbital occupations and Mulliken charge on An for the $f^0$ actinyls

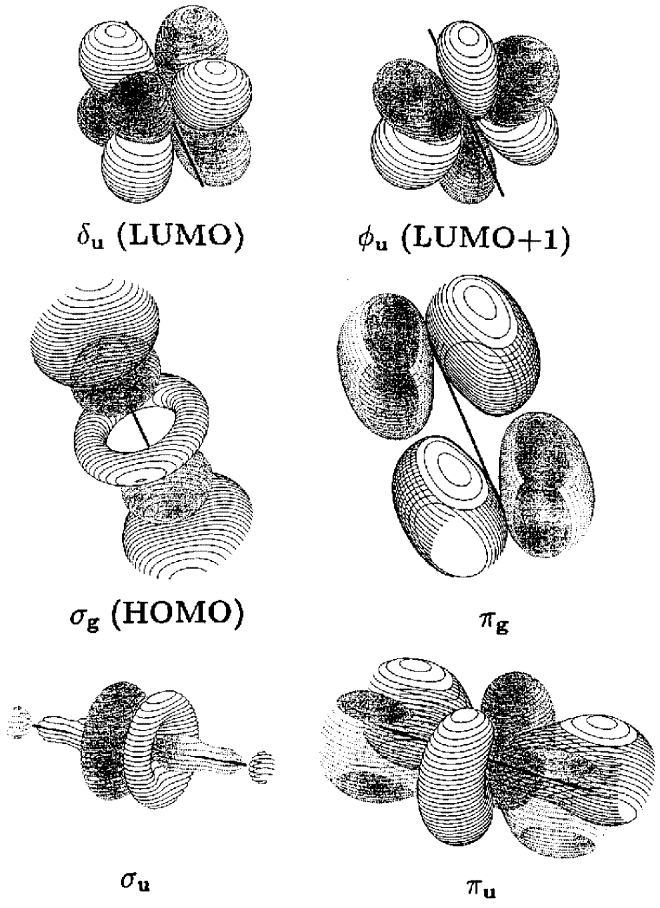


**Fig. 5.** The valence bonding and lowest unoccupied orbitals in $f^0$ actinyls

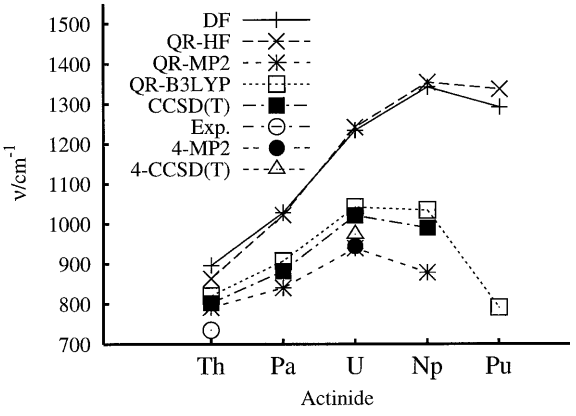


**Fig. 6.** Symmetric stretching vibrational modes for the $f^0$ actinyls

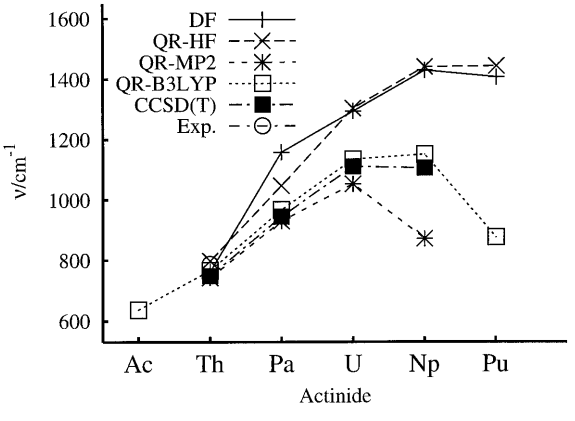


**Fig. 7.** Antisymmetric stretching vibrational modes for the $f^0$ actinyls

**Table 2.** Calculated harmonic frequencies for $AnO_2^{n+}$ ($cm^{-1}$)

| Method | $ThO_2$ | | | $PaO_2^+$ | | | $UO_2^{2+}$ | | | $NpO_2^{3+}$ | | | $PuO_2^{4+}$ | | |
|---|---|---|---|---|---|---|---|---|---|---|---|---|---|---|---|
| | $b_2$ | $a_1$ | $a_1$ | $\sigma_u$ | $\sigma_g$ | $\pi_u$ | $\sigma_u$ | $\sigma_g$ | $\pi_u$ | $\sigma_u$ | $\sigma_g$ | $\pi_u$ | $\sigma_u$ | $\sigma_g$ | $\pi_u$ |
| RLC[a] | | | | | | | | | | | | | | | |
| SCF | 781 | 843 | 177 | 1055 | 1025 | 146 | 1285 | 1234 | 284 | 1420 | 1348 | 314 | 1364 | 1278 | 267 |
| B3LYP | 756 | 788 | 100 | 981 | 933 | 159 | 1124 | 1038 | 178 | 1085 | 987 | 170 | | | |
| MP2 | 719 | 768 | 162 | 927 | 866 | 111 | 1029 | 922 | 187 | 764 | 675 | 84 | | | |
| CCSD(T) | 725 | 779 | 163 | 949 | 904 | 97 | 1095 | 1013 | 208 | 1097 | 982 | 154 | | | |
| RSC[b] | | | | | | | | | | | | | | | |
| SCF | 798 | 863 | 179 | 1047 | 1022 | 214 | 1304 | 1242 | 277 | 1441[i] | 1354 | 302 | 1444 | 1337 | 261 |
| B3LYP | 766 | 820 | 156 | 967 | 907 | 115 | 1135 | 1042 | 176 | 1151 | 1034 | 135 | 876 | 791 | 73 |
| MP2[d] | 748 | 798 | 166 | 936 | 847 | 118 | 1052 | 941 | 164 | 879 | 900 | 106 | | | |
| MP2[e] | 742 | 791 | 169 | 930 | 840 | 135 | 1053 | 939[f] | 172 | 871 | 878 | 115 | | | |
| CCSD(T) | 748[h] | 802[h] | 166 | 945 | 882 | 141 | 1111[g] | 1021[f] | 201 | 1106 | 990 | 141 | | | |
| All electron[c] | | | | | | | | | | | | | | | |
| DF | 761 | 896 | 130 | 1158 | 1028 | 130 | 1294 | 1234 | 246 | 1429 | 1342 | 268 | 1407 | 1292 | 208 |

[a] Basis set: An(RLC + 2*g*) + O(aug-cc-PVDZ)
[b] Basis set: An(RSC + 2*g*) + O(aug-cc-PVDZ)
[c] Basis set of aug-cc-PVDZ quality on both An and O
[d] Oxygen 1*s* not correlated
[e] Oxygen 1*s* and An 5*spd* not correlated
[f] The 4-MP2 and 4-CCSD(T) $\sigma_g$ are 944 and 974 $cm^{-1}$, respectively [58]
[g] The Ar matrix spectroscopy $\sigma_u$ was 952 $cm^{-1}$ [21]
[h] The Ar matrix spectroscopy data are $b_2 = 787$ and $a_1 = 735\,cm^{-1}$, respectively [17]
[i] The calculated $\sigma_u$ is 1441 $cm^{-1}$ [41]

**Table 3.** A comparison of uranyl(VI) and neptunyl(VII) symmetric and asymmetric stretching frequencies $\sigma_g$ and $\sigma_u$, respectively, ($cm^{-1}$)

| Systems | $\sigma_g$ | $\sigma_u$ | Comments |
|---|---|---|---|
| Experimental | | | |
| Uranyl salts (typical values) | 840–890 | 930–960 | [7] |
| $NpO_2(OH)_3 \cdot nH_2O$(s) | 830 | 897 | [39] |
| $NpO_2^{3+}$(aq) | 853 (25) | | [39] |
| Theoretical B3LYP (gas state)[a] | | | |
| $UO_2^{2+}$ | 1042 | 1135 | |
| $NpO_2^{3+}$ | 1034 | 1151 | |
| $UO_2F_3^-$ | 853 | 921 | |
| $NpO_2F_3$ | 918 | 1024 | |
| $UO_2F_4^{2-}$ | 799 | 860 | |
| $NpO_2F_4^-$ | 861 | 964 | |

[a] Free ion B3LYP RSC values (see Tables 2, 7)

$NpO_2F_4^-$ values are comparable with the available experimental data.

### 2.2 Oxyfluorides

The possible $f^0$ actinyl fluorides were enumerated in Fig. 1. The experimentally known ones are framed. The best chances for new species lie along the shoreline of this "island of stability". It should be added that the absence of certain data could be caused by the low desirability of the experiment, owing to toxicity, radioactivity, short life time, or cost. Small-core B3LYP structures of the actinyl oxyfluorides are shown in Tables 4 and 5 and in Figs. 2, 8 and 9. The vibrational frequencies are shown in Tables 6 and 7 and Figs. 10 and 11. The lowest curve in Fig. 8 corresponds to the actinyls, with a minimum at Np. The successive addition of one to five more equatorial fluorines to it, maintaining the $f^0$ electronic structure, leads to a relatively moderate increase in the An–O distance. The An–F distances for $[AnO_2F_n]^q$, $n = 1 - 5$, as function of $n$ are shown in Fig. 9. Again, higher An have shorter distances for the same $n$. Increasing $n$ will slightly lengthen the An–F distance. The trends are very systematic and neither encourage nor discourage the search for further species. Such conclusions must rather be based on energies. The $\sigma_u$ frequencies in Fig. 11 show an equally systematic behavior as the distances. Now some experimental frequencies are available, (Tables 6, 7). The aqueous frequencies are not directly comparable with our gas-phase values; however, they show reasonable agreement. The calculated frequencies and their trends, especially for the two An–O stretching frequencies, should aid in experimental identification of further species. Just as $ThO_2$ has a lower symmetry than $UO_2^{2+}$, we here have $C_s$ symmetry for $ThO_2F^-$, compared with $C_{2v}$ symmetry for isoelectronic $PaO_2F$ or $UO_2F^+$, (Table 4). Another possible example of the effect of small 5*f*-level excitation energies is the large deviation between B3LYP and MP2 for the $a_{1g}(\sigma_g)$ vibration of $PuO_2F_4$ (Table 7). The possible new neutral species comprise here $NpO_2F_3$ ($D_{3h}$) and $PuO_2F_4$ ($D_{4h}$). Their high symmetry may increase their chemical stability. The Pu(VIII) species is discussed in more detail later. The $D_{5h}$ species, $AmO_2F_5$ in Table 5, would be a first candidate for an Am(IX) species. The single imaginary frequency (bending of fluorines) may be a density functional theory artifact. If it is a real effect, it may indicate a lower symmetry or fluorine elimination.

**Table 4.** Calculated bond lengths (pm) and angles (degrees) for $[AnO_2F_n]^q$ species

| Systems | | Method | $r$(An–O) | $r$(An–F) | O–An–O | O–An–F | F–An–F |
|---|---|---|---|---|---|---|---|
| $C_s$ | $ThO_2F^-$ | B3LYP | 197.0 | 228.2 | 116 | 109 | |
| | | MP2 | 198.6 | 227.1 | 113 | 109 | |
| $C_{2v}$ | $PaO_2F$ | B3LYP | 185.2 | 213.8 | 159 | 100 | |
| | | MP2 | 186.7 | 213.9 | 160 | 100 | |
| | $UO_2F^+$ | B3LYP | 173.1 | 200.0 | 170 | 95 | |
| | | MP2 | 176.0 | 199.6 | 174 | 93 | |
| | $PaO_2F_2^-$ | B3LYP | 190.6 | 221.7 | 148 | | 107 |
| | | MP2 | 191.0 | 221.6 | 153 | | 110 |
| | $UO_2F_2$ | B3LYP | 176.8 | 207.5 | 168 | | 114 |
| | | MP2 | 179.4 | 207.0 | 169 | | 112 |
| | $NpO_2F_2^+$ | B3LYP | 171.3 | 197.5 | 180 | | 180 |
| | | MP2 | 173.9 | 198.5 | 180 | | 111 |

**Table 5.** Calculated bond lengths (pm) and angles (degrees) for $[AnO_2F_n]^q$ and $[AnO_5]^q$ species

| Systems | | Method | $r$(An–O) | $r$(An–F) |
|---|---|---|---|---|
| $D_{3h}$ | $PaO_2F_3^{2-}$ | B3LYP | 192.3 | 231.0 |
| | | MP2 | 192.8 | 230.3 |
| | $UO_2F_3^-$ | B3LYP | 179.0 | 216.1 |
| | | MP2 | 181.1 | 215.6 |
| | $NpO_2F_3$ | B3LYP | 173.1 | 205.9 |
| | | MP2 | 174.7 | 205.8 |
| | | HF | 164.7 | 205.9 |
| | $NpO_5^{3-}$ | HF | 173.2, 198.0 | |
| | $PuO_5^{2-}$ | B3LYP | 184.1, 195.8 | |
| $D_{4h}$ | $UO_2F_4^{2-}$ | B3LYP | 181.9 | 223.3 |
| | | MP2 | 183.9 | 222.3 |
| | $NpO_2F_4^-$ | B3LYP | 175.9 | 211.0 |
| | | MP2 | 176.2 | 211.4 |
| | $PuO_2F_4$ | B3LYP | 172.6 | 202.4 |
| | | MP2 | 173.9 | 204.7 |
| | | HF | 162.4 | 200.3 |
| | $PuO_6^{4-a}$ | HF | 172.3 | 190.0 |
| $D_{5h}$ | $NpO_2F_5^{2-}$ | B3LYP | 176.9 | 220.6 |
| | | MP2 | 176.3 | 220.7 |
| | $PuO_2F_5^-$ | B3LYP | 173.5 | 212.6 |
| | | MP2 | 174.4 | 215.1 |
| | $AmO_2F_5$ | B3LYP | 171.4 | 208.4 |

[a] Counterion charges added

### 2.2.1 The $AnO_5^q$ species

Starting with $NpO_2F_3$ and replacing the fluorine atoms by $O^-$ we arrive at $NpO_5^{3-}$. This species is experimentally known in the solid state as $NpO_2(OH)_3 \cdot nH_2O$ [38]. Its HF structure is shown in Table 5. Compared with the neutral $NpO_2F_3$, the two axial Np–O distances are lengthened by 8 pm. The equatorial Np–O distances are shorter than the equatorial Np–F distances. Also the stretching frequencies of axial oxygen bonding are smaller for $NpO_5^{3-}$ than for the $NpO_2F_3$ analogues. This may suggest a ''resonance'' between axial and equatorial Np–O bonds. No counterions were included at this HF calculation. The predicted structure and vibrational frequencies are new. The hypothetical plutonium analogue is included in Tables 5 and 7.

### 2.2.2 Equatorial bonding

Coulson and Lester [39] suggested that the equatorial bonding of $UO_2(NO_3)_3^-$ would take place between the U

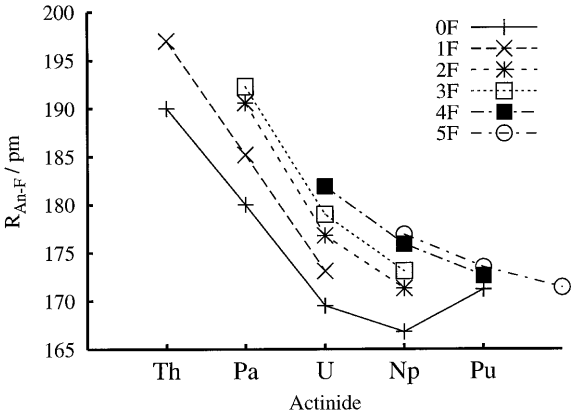


**Fig. 8.** The trends in calculated B3LYP An–O distances for the $[AnO_2F_n]^q$ species

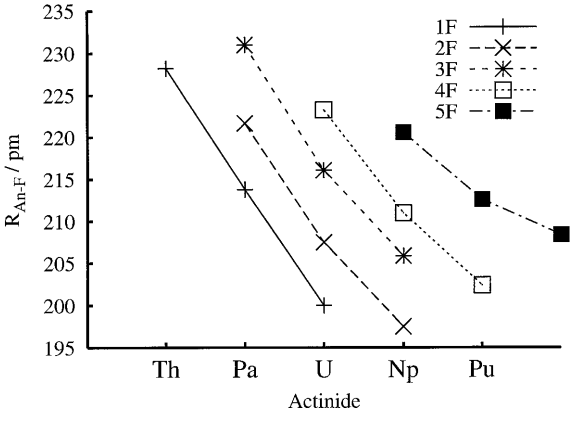


**Fig. 9.** The trends in calculated B3LYP An–F distances for the $[AnO_2F_n]^q$ species

$5f\phi$ orbital and the nitrate oxygens. No evidence for this was found at the HF ab initio level by Pyykkö et al. [1]. The total $5f\phi_U - 2p_F$ overlap populations were about 0.03, only. We now find examples of $5f\phi$ involvement in equatorial bonding. For $UO_2F_3^-$, $UO_2F_4^{2-}$, $NpO_2F_3$, $NpO_2F_4^-$ and $NpO_2F_5^{2-}$ the Mulliken overlap populations are 0.11, 0.03, 0.16, 0.24 and 0.21, respectively. A closer look at the specific MOs in Fig. 12 makes this covalent involvement quite evident. This suggests rehabilitation of Coulson's idea but in different systems than the uranyl trinitrate originally considered in 1956.

### 2.3 Pu(VIII)?

In addition to $PuO_2F_4$, we studied neutral $PuO_4$ and $PuF_8$. Their calculated properties are shown in Table 8. As seen here, the $PuO_4$ bond distance is longer than the $PuO_2^{4+}$ one by about 5 pm at the QR-B3LYP level. There are very large apparent correlation effects at the MP2 level for $PuO_4$ and the T1 diagnostic for CCSD(T) is quite large (T1 = 0.06 at the minimum geometry), Also at the B3LYP level, the $D_{4h}$ system tends to slightly bend to $D_{2d}$, with minimal changes in energy, distance and frequencies. The reasons are similar to those discussed in Sect. 2.1. Owing to the strong multiconfigurational character, the very existence of $PuO_4$ is somewhat questionable, although good minima are found at different levels. Parenthetically, the isoelectronic "anti-uranyl" group $UO_4^{2-}$ [40] and "antineptunyl" groups are known and possess $D_{4h}$ symmetries in crystals (Fig. 4 in Ref. [1]). For free $UO_4^{2-}$ in a vacuum, Bolvin et al. (to be published) calculated a $T_d$ structure, while free $NpO_4^-$ was found to be $D_{4h}$, like our $PuO_4$. They concluded that it is the availability of $f$ orbitals for bonding which participate in covalent bonding of Np that drive $NpO_4^-$ to the $D_{4h}$ geometry.

The valence isoelectronic $NpO_3F$ has been observed thermochromatographically [27] and its calculated $C_{2v}$ structure (quasi $D_{4h}$) resembles that of $PuO_4$ (Table 8).

For $PuF_8$ a cubic $O_h$ structure was found. The $D_{4d}$ alternative (tetragonal antiprism) was a transition state. The Pu–F distance is surprisingly close to the experimental An–F distance for $UF_6$ (199.6 pm) [41] or $PuF_6$ (197.1 pm) [41]. This suggests a sturdy structure. We are unaware of earlier discussions of $PuF_8$. The $PuO_3F_2$ system was unstable as $D_{3h}$ or $C_{2v}$ systems, and we did not study it in more detail.

#### 2.3.1 Thermochemistry

How high do these compact, sturdy Pu(VIII) species lie? In order to have a thermochemical reference point, we calculated the Pu(VI) system $PuF_6(O_h)$ at the B3LYP level. We assumed an $^1A_{1g}$ state with two $f$ electrons in the $a_{2u}$ orbital, which is the ground state of the molecule. According to Ref. [42], the order of the $5f$ levels in $PuF_6$ is $a_{2u} < t_{1u} < t_{2u}$. Then, for the following hypothetical reactions, the B3LYP energies, without any vibrational corrections, are

$$PuF_6 + F_2 \rightarrow PuF_8 \quad \Delta E = 274\,\text{kJ/mol} \tag{1}$$

$$PuF_6 - F_2 + O_2 \rightarrow PuO_2F_4 \quad \Delta E = 514\,\text{kJ/mol} \tag{2}$$

$$PuF_6 - 3F_2 + 2O_2 \rightarrow PuO_4 \quad \Delta E = 1243\,\text{kJ/mol} \tag{3}$$

The calculated gas-phase standard enthalpies are 281, 515 and 1239 kJ/mol, respectively. We repeat that although "uphill", $PuF_8$, $PuO_2F_4$ and $PuO_4$ are local minima with clearly positive vibrational frequencies. Another reference point could be the $PuO_2F_2$ molecule, which was found to be triplet $^3B_2$ in the ground state (at the B3LYP level). Without any vibrational corrections, the B3LYP energies are

$$PuO_2F_2 + 3F_2 - O_2 \rightarrow PuF_8 \quad \Delta E = -427\,\text{kJ/mol} \tag{4}$$

$$PuO_2F_2 + F_2 \rightarrow PuO_2F_4 \quad \Delta E = -182\,\text{kJ/mol} \tag{5}$$

$$PuO_2F_2 - F_2 + O_2 \rightarrow PuO_4 \quad \Delta E = 547\,\text{kJ/mol} \tag{6}$$

The calculated gas-phase standard enthalpies are −413, −179 and 544 kJ/mol, respectively. Thus, this would be the order of the thermochemical accessibility of these three species. This is confirmed by DF calculations on the reactions

$$Pu + 2F_2 + O_2 \rightarrow PuO_2F_4 \quad \Delta E = -919\,\text{kJ/mol} \tag{7}$$

$$Pu + 2O_2 \rightarrow PuO_4 \quad \Delta E = 776\,\text{kJ/mol} \tag{8}$$

One possibility to make $PuO_2F_4$ would be the neutron irradiation of $[^{238}UO_2F_4]^{2-}$ compounds.

$$^{238}_{92}U \xrightarrow{+n} {}^{239}_{92}U \xrightarrow{-\beta} {}^{239}_{93}Np \xrightarrow{-\beta} {}^{239}_{94}Pu \tag{9}$$

This is the familiar nuclear reaction producing large quantities $^{239}Pu$ in normal power reactors [37]. Similarly,

**Table 6.** Calculated harmonic vibrational modes ($cm^{-1}$) for $[AnO_2F_n]^q$species

| Systems | Frequencies | | | | | | | | | |
|---|---|---|---|---|---|---|---|---|---|---|
| $C_s$ | Method | $a'$ | $a''$ | $a'$ | $a'$ | $a''$ | $a'$ | | | |
| $ThO_2F^-$ | B3LYP | 742 | 663 | 399 | 178 | 139 | 108 | | | |
| | MP2 | 724 | 650 | 411 | 179 | 139 | 114 | | | |
| $C_{2v}$ | Method | $b_2$ | $a_1$ | $a_1$ | $a_1$ | $b_2$ | $b_1$ | | | |
| $PaO_2F$ | B3LYP | 858 | 820 | 511 | 177 | 160 | 146 | | | |
| | MP2 | 852 | 789 | 519 | 168 | 159 | 131 | | | |
| $UO_2F^+$ | B3LYP | 1049 | 970 | 634 | 129 | 201 | 180 | | | |
| | MP2 | 999 | 898 | 648 | 111 | 219 | 141 | | | |
| $C_{2v}$ | Method | $b_2$ | $a_1$ | $a_1$ | $b_1$ | $b_1$ | $a_2$ | $a_1$ | $b_2$ | $a_1$ |
| $PaO_2F_2^-$ | B3LYP | 760 | 756 | 443 | 429 | 186 | 170 | 147 | 160 | 87 |
| | MP2 | 771 | 750 | 450 | 439 | 190 | 176 | 163 | 162 | 87 |
| $UO_2F_2$ | B3LYP | 971[a] | 903 | 559 | 544 | 240 | 220 | 213 | 203 | 81 |
| | MP2 | 942 | 849 | 568 | 555 | 212 | 218 | 182 | 205 | 90 |
| $NpO_2F_2^+$ | B3LYP | 1071 | 961 | 597 | 640 | 302 | 271 | 197 | 211 | 85 |
| | MP2 | 1034 | 1024 | 657 | 642 | 224 | 226 | 223 | 216 | 67 |

[a] The Ar matrix spectroscopy value is 940 $cm^{-1}$ [23]

**Table 7.** Calculated harmonic vibrational modes ($cm^{-1}$) for $[AnO_2F_n]^q$ and $[AnO_5]^q$ species

| Systems | Frequencies | | | | | | | | | | | |
|---|---|---|---|---|---|---|---|---|---|---|---|---|
| $D_{3h}$ | Method | $a_2''$ | $a_1'$ | $a_1'$ | $e'$ | $e'$ | $e''$ | $a_2''$ | $e'$ | | | |
| $PaO_2F_3^{2-}$ | B3LYP | 735 | 715 | 353 | 350 | 228 | 217 | 165 | 71 | | | |
| | MP2 | 742 | 721 | 366 | 363 | 224 | 216 | 166 | 75 | | | |
| $UO_2F_3^-$ | B3LYP | 921 | 853 | 470 | 459 | 266 | 238 | 179 | 86 | | | |
| | MP2 | 910 | 819 | 477 | 468 | 243 | 240 | 184 | 91 | | | |
| $NpO_2F_3$ | B3LYP | 1024 | 918 | 563 | 552 | 285 | 234 | 175 | 63 | | | |
| | MP2 | 1048 | 1036 | 578 | 561 | 251 | 229 | 175 | 69 | | | |
| $NpO_2F_3$ | B3LYP | 1024 | 918 | 563 | 552 | 285 | 234 | 175 | 63 | | | |
| | MP2 | 1048 | 1036 | 578 | 561 | 251 | 229 | 175 | 69 | | | |
| | HF | 1242 | 1166 | 592 | 575 | 386 | 278 | 204 | 110 | | | |
| $NpO_5^{3-}$ | HF | 982 | 863 | 579 | 452 | 378 | 347 | 302 | 140 | | | |
| $PuO_5^{2-}$ | B3LYP | 768 | 739 | 522 | 551 | 305 | 282 | 239 | 55*i* | | | |
| $D_{4h}$ | Method | $a_{2u}$ | $a_{1g}$ | $a_{1g}$ | $e_u$ | $b_{1g}$ | $e_u$ | $e_g$ | $a_{2u}$ | $b_{2g}$ | $b_{2u}$ | $e_u$ |
| $UO_2F_4^{2-}$ | B3LYP | 860[a] | 799[b] | 402[b] | 382[a] | 344 | 267 | 247 | 192 | 163 | 145 | 112 |
| | MP2 | 861 | 778 | 411 | 393 | 358 | 246 | 242 | 186 | 169 | 142 | 119 |
| $NpO_2F_4^-$ | B3LYP | 964 | 861 | 500 | 493 | 434 | 290 | 248 | 198 | 182 | 149 | 136 |
| | MP2 | 1020 | 996 | 507 | 498 | 427 | 261 | 237 | 188 | 181 | 144 | 137 |
| $PuO_2F_4$ | B3LYP | 1011 | 880 | 553 | 572 | 494 | 287 | 228 | 210 | 201 | 156 | 151 |
| | MP2 | 1142 | 1281 | 548 | 568 | 520 | 258 | 201 | 170 | 200 | 124 | 161 |
| $D_{5h}$ | Method | $a_2''$ | $a_1'$ | $a_1'$ | $e_1'$ | $e_2'$ | $e_1'$ | $e_2'$ | $e_1''$ | $a_2''$ | $e_1'$ | $e_2''$ |
| $NpO_2F_5^{2-}$ | B3LYP | 934 | 826 | 437 | 385 | 319 | 302 | 272 | 252 | 191 | 176 | 68 |
| | MP2 | 1011 | 980 | 447 | 387 | 314 | 279 | 272 | 238 | 181 | 183 | 56 |
| $PuO_2F_5^-$ | B3LYP | 989 | 855 | 495 | 451 | 387 | 306 | 286 | 241 | 195 | 169 | 32*i* |
| | MP2 | 1146 | 1238 | 482 | 445 | 373 | 265 | 259 | 162 | 146 | 141 | 105*i* |
| $AmO_2F_5$ | B3LYP | 1015 | 859 | 510 | 460 | 403 | 297 | 272 | 198 | 194 | 117 | 108*i* |

[a] Experimental aqueous IR values are 920 $cm^{-1}$ for the $a_{2u}$ asymmetric U–O stretch and 370 $cm^{-1}$ for the U–F stretching frequency
[b] Experimental solid state Raman values are 940 $cm^{-1}$ for the $a_{1g}$ symmetric U–O stretching and 370 $cm^{-1}$ for the U–F stretching

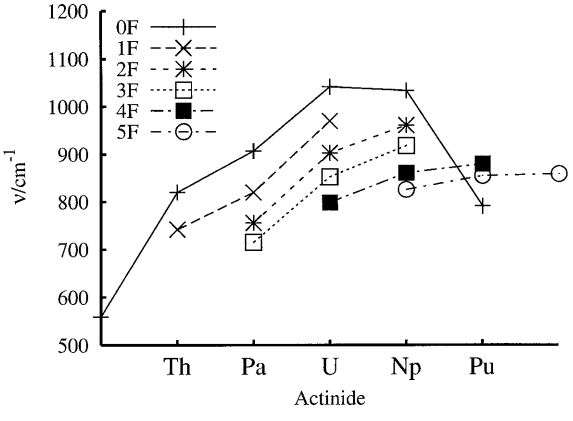


**Fig. 10.** The trends in calculated B3LYP symmetric stretching vibrational modes of the An–O bond for $[AnO_2F_n]^q$ species

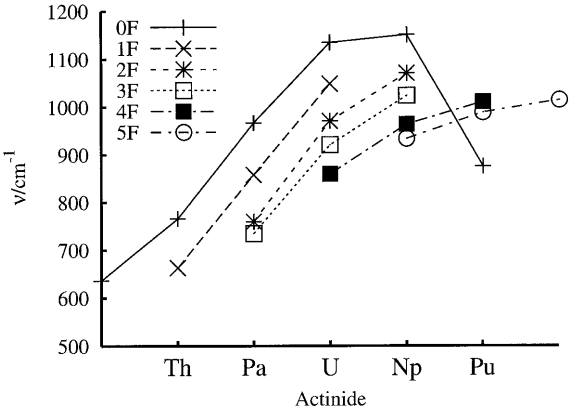


**Fig. 11.** The trends in calculated B3LYP asymmetric stretching vibrational modes of the An–O bond for $[AnO_2F_n]^q$ species

the neutron irradiation of an "antiuranyl" compound such as $Na_4UO_5$ could, in principle, yield $PuO_4$. In other words, we suggest carrying out the chemical reaction before the nuclear reaction. In matrix spectroscopy, if the molecule $Pu^{VI}OF_4$ could be produced first, the reaction with an O atom might afford $PuO_2F_4$. Note that $PuOF_4$ was observed in Ref. [27]. The observation of Pu(VIII) might take place through spectroscopy or through heating or sputtering and subsequent mass-spectroscopy, or by thermochromatography.

There are several other possibilities for making these compounds. One is direct fluorination of $PuF_6$ or $PuO_2F_2$ to produce $PuF_8$ and $PuO_2F_4$, and perhaps O-atom or ion bombardment of plutonium oxides to generate $PuO_4$. Another interesting possibility which would initially produce Pu(VII) is negative ion photoelectron spectroscopy. Here the ions $PuF_8^-$, $PuO_2F_4^-$ or $PuO_4^-$ would be generated in the gas phase, ion-selected in a mass spectrometer and then neutralized by photodetachment or otherwise. The photoelectron spectrum would give information about oxidation state VIII: a discrete spectrum would indicate a stable neutral species. Experimental thermochromatographic studies give evidence for volatile $Pu^{VI}OF_4$ and $Pu^{VII}O_3F$ [27].

### 2.3.2 Cubic versus antiprism structures

$PuF_8$ was found here to be cubic, $O_h$. Experimentally, Hwang and Seppelt [37] found that isoelectronic $UF_8^{2-}$ in crystalline $(NO)_2(UF_8)$ has an antiprism, $D_{4d}$ structure with U–F(av) = 210.2 pm. Our calculated RSC B3LYP value is 213 pm for the $D_{4d}$ structure. All frequencies are positive. The $O_h$ structure is a transition state with one imaginary double degenerate frequency ($e_u$), which corresponds to rotation from the cube to an antiprism. The $NpF_8^-$ was found to be cubic, like $PuF_8$. The antiprism $NpF_8^-$ and $PuF_8$ have one imaginary frequency ($b_1$), corresponding to rotation of the antiprism to a cube. The energy difference $E(O_h) - E(D_{4d})$ is 19, −7 and −26 kJ/mol for $UF_8^{2-}$, $NpF_8^-$, and $PuF_8$, respectively. Note the shortening of the An–F distance along the series in Table 8.

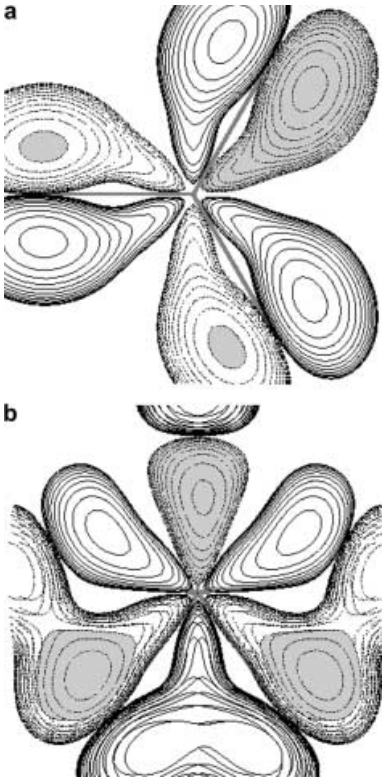


**Fig. 12.** Selected molecular orbitals of **a** $UO_2F_3^-$ and **b** $NpO_2F_5^{2-}$ HOMO-7 and HOMO-10, respectively

### 2.3.3 A symmetry trend

In addition to the symmetry change from $ThO_2F^-(C_s)$ to $PaO_2F$ ($C_{2v}$), we notice the systematic trend in Table 10. On each row the calculated symmetry of the molecule changes. Left of the vertical line the inversion symmetry is missing; right of the vertical line it exists. The driving force behind this change must be left to future investigation. A possible mechanism could be the constant 6*d* orbital energies as contrasted to the increasingly stabilized 5*f* orbital energies along the actinide series (Th–Am) [43].

## 3 Conclusions

1. Geometries and vibrational spectra for a number of novel, experimentally unknown $f^0d^0$ gas-phase actinyl fluoride species were calculated. For most of the known species, the geometries and vibrational spectra were reported for the first time.
2. The gas-phase species $ONpO^{3+}$ is likely to exist. It should have a slightly shorter bond length and similar vibrational frequencies, compared with free $UO_2^{2+}$. Its neutral derivative, $NpO_2F_3$ is a possible new neutral species.

**Table 8.** Bond lengths (pm) and selected frequencies ($cm^{-1}$) for Pu(VIII) systems and some related cases

| System | Symm | Method | *r*(Pu–O) | *r*(Pu–F) | Pu–O stretching | | | Pu–F stretching | | | |
|---|---|---|---|---|---|---|---|---|---|---|---|
| $PuO_4$ | $D_{4h}$ | DF | 172.3 | | 1014 ($e_u$) | 974 ($a_{1g}$) | 733 ($b_{1g}$) | | | | |
| | $D_{4h}$ | HF | 169.5 | | 1060 ($e_u$) | 1046 ($a_{1g}$) | 833 ($b_{1g}$) | | | | |
| | $D_{4h}$ | B3LYP | 176.6 | | 920 ($e_u$) | 873 ($a_{1g}$) | 735 ($b_{1g}$) | | | | |
| | $D_{2d}$[a] | B3LYP | 176.6 | | 912 ($e$) | 862 ($a_1$) | 728 ($b_2$) | | | | |
| | $D_{4h}$ | MP2 | 175.4 | | 1026 ($e_u$) | 1140 ($a_{1g}$) | 1050 ($b_{1g}$) | | | | |
| | $D_{4h}$ | CCSD(T) | 177.7 | | | | | | | | |
| $NpO_3F$ | $C_{2v}$[b] | B3LYP | 176.2, 180.5 | 204.6 | 954 ($a''$) | 893 ($a'$) | 796 ($a'$) | 526 ($a'$) | | | |
| $PuO_2F_4$ | $D_{4h}$ | DF | 164.1 | 199.3 | 1232 ($a_{2u}$) | 1122 ($a_{1g}$) | | 631 ($e_u$) | 610 ($a_{1g}$) | 504 ($b_{1g}$) | |
| | $D_{4h}$ | HF | 162.4 | 200.3 | 1284 ($a_{2u}$) | 1165 ($a_{1g}$) | | 618 ($e_u$) | 615 ($a_{1g}$) | 495 ($b_{1g}$) | |
| | $D_{4h}$ | B3LYP | 172.6 | 202.4 | 1011 ($a_{2u}$) | 880 ($a_{1g}$) | | 287 ($e_u$) | 553 ($a_{1g}$) | 494 ($b_{1g}$) | |
| $PuF_8$ | $O_h$ | HF | | 192.9 | | | | 702 ($a_{1g}$) | 671 ($t_{1u}$) | 458 ($t_{2g}$) | 522 ($b_{2u}$) |
| | | B3LYP | | 200.9 | | | | 589 ($a_{1g}$) | 567 ($t_{1u}$) | 454 ($t_{2g}$) | 434 ($b_{2u}$) |
| | $D_{4d}$ | B3LYP | | 202.4 | | | | 593 ($a_1$) | 544 ($b_2$) | 535 ($e_2$) | 463 ($e_2$) |
| | | | | | | | | 446 ($e_2$) | | | |
| $NpF_8^-$ | $O_h$ | B3LYP | | 206.0 | | | | 581 ($a_{1g}$) | 525 ($t_{1u}$) | 425 ($t_{2g}$) | 395 ($b_{2u}$) |
| | $D_{4d}$ | B3LYP | | 206.6 | | | | 587 ($a_1$) | 509 ($b_2$) | 508 ($e_2$) | 433 ($e_2$) |
| | | | | | | | | 420 ($e_2$) | | | |
| $UF_8^{2-}$ | $O_h$ | B3LYP | | 213.1 | | | | 544 ($a_{1g}$) | 450 ($t_{1u}$) | 366 ($t_{2g}$) | 323 ($b_{2u}$) |
| | $D_{4d}$ | B3LYP | | 213.3 | | | | 550 ($a_1$) | 442 ($b_2$) | 446 ($e_2$) | 375 ($e_2$) |
| | | | | | | | | 358 ($e_2$) | | | |

[a] Slight distortion O–Pu–O bends to 175°
[b] Calculated as a $C_s$ system

**Table 9.** Calculated bond lengths (pm) and frequencies ($cm^{-1}$) for Pu(VI) systems

| System | Symmetry | State | Method | $r$(Pu–O) | $r$(Pu–F) | Pu–O stretching | | Pu–F stretching | | |
|---|---|---|---|---|---|---|---|---|---|---|
| $PuF_6$ | $O_h$ | $^1A_{1g}$ | B3LYP | | 197.4 | | | 640 ($a_{1g}$) | 612 ($t_{1u}$) | 523 ($e_g$) |
| $PuF_6$ | $O_h$ | $^1A_{1g}$ | Exp.[a] | | 197.1 | | | 628 ($a_{1g}$) | 617 ($t_{1u}$) | 503 ($e_g$) |
| $PuOF_4$ | $C_{4v}$ | $^1A_{1g}$ | B3LYP | 176.8 | 200.8 | 864 ($a_1$) | | 585 ($a_1$) | 576 ($e$) | 507 ($b_2$) |
| $PuO_2F_2$ | $C_{2v}$ | $^1A_{1g}$ | B3LYP | 172.4 | 204.0 | 988 ($b_2$) | 901 ($b_2$) | 564 ($a_1$) | 543 ($b_1$) | |
| $PuO_2F_2$ | $C_{2v}$ | $^3B_2$ | B3LYP | 173.7 | 206.2 | 977 ($b_2$) | 875 ($b_2$) | 557 ($a_1$) | 540 ($b_1$) | |
| $PuO_2F_4^{2-}$ | $D_{4h}$ | $^1A_{1g}$ | B3LYP | 177.0 | 220.5 | 886 ($a_{2u}$) | 797 ($a_{1g}$) | 401 ($a_{1g}$) | 381 ($e_u$) | 339 ($b_{1g}$) |
| $PuO_3$ | $C_{2v}$ | $^1A_{1g}$ | B3LYP | 181.1, 175.2 | | 912 ($b_2$)<br>776 ($a_1$) | 880 ($a_1$) | | | |

[a] Ref. [41]

**Table 10.** Examples of symmetry change

| Class | ⇐ No inversion | Inversion ⇒ |
|---|---|---|
| $AnO_2^q$ | $ThO_2$ | $PaO_2^+$ $UO_2^{2+}$ $NpO_2^{3+}$ |
| | $C_{2v}$ | $D_{\infty h}$ |
| $AnO_4^q$ | $UO_4^{2-}$ | $NpO_4^-$ $PuO_4$ |
| | $T_d$ | $D_{4h}$ |
| $AnF_8^q$ | $UF_8^{2-}$ | $NpF_8^-$ $PuF_8$ |
| | $D_{4d}$ | $O_h$ |

3. In actinyl systems with equatorial ligands, the experimental $\sigma_g$ and $\sigma_u$ An–O stretching vibrations are comparable for $U^{VI}O_2L_n$ and $Np^{VII}O_2L_n$ systems. This trend is supported by the present calculation.
4. The structures of the experimentally known $NpO_5^{3-}$ and $NpO_3F$ were calculated.
5. $PuF_8(O_h)$, $PuO_2F_4(D_{4h})$ and possibly $PuO_4(D_{4h})$ are new high-energy species. All of them contain the so far unknown Pu(VIII).
6. The $D_{4d}$ geometry of solid-state $UF_8^{2-}$ seems to be internally driven; it was calculated to be $D_{4d}$ in the gas phase. In contrast, $NpF_8^-$ and $PuF_8$ are cubic ($O_h$) systems. $PuF_8$ is an interesting molecule because it might be the first Pu(VIII) species and the first neutral cubic ($O_h$) $XY_8$ molecule at the same time.

## 4 Methodology

Several studies on the methodology for actinide species calculations can be found in the literature [32, 44–48]. Our indicative calibration of the QR pseudopotential (ECP) treatment is available [49]. There we calculated the $UF_6, UO_2F_2, UO_2^{2+}$ and $ThO_2$ molecules, for which experimental and high-level calculation results exist. In our calculations, we tested small core (RSC) and large core (RLC) pseudopotentials [50] on the structures and harmonic vibrational frequencies using methods from HF to CCSD(T). Furthermore we varied the basis sets for O and F and studied the importance of g functions on An. An illustrative part is in Sect. 2.1, where we compared large core (RLC) and small core (RSC) pseudopotentials [50], and the methods from HF to CCSD(T).

For dioxoactinide calculations the aug-cc-PVDZ basis set on O was used. In oxyfluoride calculations the small core ECPs [50] (RSC) for actinides, augmented by two g functions with exponents $\alpha_1 = 1.524$, $\alpha_2 = 0.375$, were used and the aug-cc-PVDZ basis set was taken for O and F atoms. Both MP2 and density functional B3LYP methods were chosen for the production work as the deviation between these two should better indicate the reliability of the calculation. Recall that our systems are closed-shell $f^0$ species, so MP2 and B3LYP should both be relatively reliable and comparable, except in cases with very small highest occupied MO–LUMO gaps. For thermochemical estimates the aug-cc-PVTZ basis set for O and F was also tested, but the changes were minimal. QR calculations were done with the Gaussian 98 [57], Molcas-4 [52] and Turbomole [53] packages.

The DF calculations were carried out using the program suite DREAMS.[1] The basis set for O was the aug-cc-pVDZ basis [56] and the basis set for U was a double-zeta-quality basis set used previously for calculations on dioxoactinide species [30]. The O atoms were treated nonrelativistically according to the model proposed by Dyall and Enevoldsen [57]. Geometries and harmonic frequencies were obtained from numerical fits to data obtained at a range of points. The fitting functions included at least the lowest anharmonic terms.

*Acknowledgements.* This work was supported by The Academy of Finland and the graduate school LASKEMO. The calculations were performed on DEC (Compaq) Alpha Station workstations at the Department of Chemistry, University of Helsinki. Computing resources from CSC (Finland) are gratefully acknowledged. The DHF calculations were performed on the Cray T3E-900 computer at the National Energy Research Scientific Computing Center, which is supported by the Office of Energy Research of the US Department of Energy under contract no. DE-AC03-76SF00098. Nino Runeberg, Dage Sundholm and Juha Vaara made useful remarks and suggestions.

[1] DREAMS is a Dirac-based relativistic electronic atomic and molecular structure program suite, consisting of a version of MOLECULE, a vectorized integral program developed by J. Almlöf and P. R. Taylor, adapted by P. R. Taylor and K. Fægri Jr., and a Dirac–HF and MP2 program developed by K. G. Dyall. The Dirac–HF program methods are described in Ref. [54] and the MP2 program methods are described in Ref. [55].

## References


1. Pyykkö P, Li J, Runeberg N (1994) J Phys Chem 98: 4809
2. Heinemann C, Schwarz H (1995) Chem Eur J 1: 7
3. Zhou MF, Andrews L (1999) J Chem Phys 111: 11044
4. Katz JJ, Seaborg GT, Morss LR (1986) The chemistry of the actinide elements, 2nd edn. Chapman and Hall, London
5. Denning RG (1983) Gmelin handbook of inorganic chemistry U supplement A6: 31
6. Denning RG (1992) Struct Bonding 79: 215
7. Glebov VA (1983) Electronic structure and properties of uranyl compounds. Energoatomizdat, Moscow
8. Balasubramanian K (1994) In: Gschneidner KA Jr, Eyring L, Choppin GR, Lander GH (eds) Handbook on the physics and chemistry of rare earths, vol 18. Elsevier, Amsterdam, pp 29–158
9. Pepper M, Bursten BE (1991) Chem Rev 91: 719
10. Kaltsoyannis N (1997) J Chem Soc Dalton Trans 1
11. Kaltsoyannis N, Scott P (1999) The f elements. Oxford University Press, Oxford, chapter 3
12. Willetts A, Gagliardi L, Ioannou AI, Simper AM, Skylaris CK, Spencer S, Handy NC (2000) Int Rev Phys Chem 19: 327
13. Pyykkö P (2000) Relativistic theory of atoms and molecules. III. A bibliography 1993–1999. Lecture notes in chemistry. Springer, Berlin Heidelberg New York
14. http://www.csc.fi/rtam/
15. Pyykkö P, Stoll H (2000) In: Hinchliffe A (ed) In Royal Society of Chemistry specialist periodical reports. Chemical modelling, applications and theory 2000. Royal Society of Chemistry, Cambridge pp 239–305
16. Kaufman M, Muenter J, Klemperer W (1967) J Chem Phys 47: 3365
17. Gabelnick SD, Reedy GT, Chasanov MG (1974) J Chem Phys 60: 1167
18. Zhou MF, Andrews L, Li J, Bursten BE (1999) J Am Chem Soc 121: 12188
19. Katz JJ, Seaborg GT, Morss LR (1986) The chemistry of the actinide elements, 2nd edn. Chapman and Hall, London, p 1511
20. Cornehl HH, Heinemann C, Marçalo J, Pires de Matos A, Schwarz H (1996) Angew Chem Int Ed Engl 35: 891

21a. Hunt RD, Andrews L (1993) J Chem Phys 98: 3690 b. Zhou M-F, Andrews L, Ismail N, Marsden C (2000) J Phys Chem A 104: 595

22. Spitsyn VI, Gelman AD, Krot NN, Zakharova FA, Komkov YA, Shilov VP, Smirnova IV (1969) J Inorg Nucl Chem 31: 2733
23. Souter PF, Andrews L (1997) J Mol Struct (THEOCHEM) 412: 161
24. Katz JJ, Seaborg GT, Morss LR (1986) The chemistry of the actinide elements, 2nd edn. Chapman and Hall, London, p 352
25. Ferri D, Salvatore F, Vasca E, Glaser J, Grenthe I (1993) Acta Chem Scand 47: 855
26. Katz JJ, Seaborg GT, Morss LR (1986) The chemistry of the actinide elements, 2nd edn. Chapman and Hall, London, p 1428.
27. Fargeas M, Fremont-Lamouranne R, Legoux Y, Merini J (1986) J Less Common Met 121: 439
28. Vallet V, Maron L, Schimmelpfennig B, Leininger T, Teichteil C, Gropen O, Grenthe I, Wahlgren U (1999) J Phys Chem A 103: 9285
29. Matsika S, Pitzer RM (2001) J Phys Chem 105: 637, and references there in
30. Dyall KG (1999) Mol Phys 96: 511
31. Spitsyn VI, Ionova GV, Kiseleva AA (1986) Zh Neorg Khim 31: 1492
32. Schreckenbach G, Hay PJ, Martin RL (1999) J Comput Chem 20: 70
33. Kaltsoyannis N (2000) Inorg Chem 39: 6009
34. Gagliardi L, Roos BO (2000) Chem Phys Lett 331: 229
35. Pyykkö P, Runeberg N, Straka M, Dyall KG (2000) Chem Phys Lett 328: 415
36. Hwang IC, Seppelt K (2000) J Fluorine Chem 102: 69
37. Seaborg GT, Loveland WD (2000) In: Hall N (ed) The new chemistry. Cambridge University Press, Cambridge, p 21
38. Chaikhorskii AA (1971) Radiokhimiya 13: 302
39. Coulson CA, Lester GR (1956) J Chem Soc 3650
40. Pyykkö P, Zhao YF (1991) Inorg Chem 30: 3787
41. Weinstock B, Goodman GL (1965) Adv Chem Phys 9: 169
42. Hay PJ, Martin RL (1998) J Chem Phys 109: 3875
43. Pyykkö P, Laakkonen LJ, Tatsumi K (1989) Inorg Chem 28: 1801
44. Gagliardi L, Handy NC, Ioannou AG, Skylaris CK, Spencer S, Willetts A, Simper AG (1998a) Chem Phys Lett 283: 187
45. Ismail N, Heully JL, Saue T, Daudey JP, Marsden CJ (1999) Chem Phys Lett 300: 296
46. Han YK, Hirao K (2000) Chem Phys Lett 324: 453
47. Han YK, Hirao K (2000) J Chem Phys 113: 7345
48. Gagliardi L, Skylaris CK, Willetts A, Dyke JM, Barone V (2000) Phys Chem Chem Phys 2: 3111
49. http://www.chem.helsinki.fi/straka/CALIBRATION/calibration.ps
50. http://www.theochem.uni-stuttgart.de/pseudopotentiale/
51. Frisch MJ, Trucks GW, Schlegel HB, Scuseria GE, Robb MA, Cheeseman JR, Zakrzewski VG, Montgomery JA, Stratmann RE, Burant JC, Dapprich S, Millam JM, Daniels AD, Kudin KN, Strain MC, Farkas O, Tomasi J, Barone V, Cossi M, Cammi R, Mennucci B, Pomelli C, Adamo C, Clifford S, Ochterski J, Petersson GA, Ayala PY, Cui Q, Morokuma K, Malick DK, Rabuck AD, Raghavachari K, Foresman JB, Cioslowski J, Ortiz JV, Stefanov BB, Liu G, Liashenko A, Piskorz P, Komaromi I, Gomperts R, Martin RL, Fox DJ, Keith T, Al-Laham MA, Peng CY, Nanayakkara A, Gonzalez C, Challacombe M, Gill PMW, Johnson BG, Chen W, Wong MW, Andres JL, Head-Gordon M, Replogle ES, Pople JA, (1998) Gaussian 98, revision A.7. Gaussian, Pittsburgh Pa
52. Andersson K, Blomberg MRA, Fülscher MP, Lindh R, Malmqvist P-A, Neogrády P, Olsen J, Roos BO, Sadlej AJ, Schütz M, Seijo L, Serrano-Andrés L, Siegbahn PEM, Widmark PO (1997) MOLCAS, version 4. Lund University, Sweden
53. Ahlrichs R, Bär M, Häser M, Horn H, Kölmel C (1989) Chem Phys Lett 162: 165
54. Dyall KG (1994) In: Malli GL (ed) Relativistic and correlation effects in molecules and solids. Plenum, New York, p 17
55. Dyall KG (1994) Chem Phys Lett 224: 186
56. Dunning Jr TH (1989) J Chem Phys 90: 1007
57. Dyall KG, Enevoldsen T (1999) J Chem Phys 111: 10000
58. de Jong WA, Visscher L, Nieuwpoort WC (1999) J Mol Struct (THEOCHEM) 458: 41
59. Green DW, Reedy GT (1979) J Mol Spectrosc 74: 423